UDC 004.81

ANALYSIS OF HUMAN GAIT BALANCE BASED ON PLANTAR PRESSURE SENSORS

HAO LI

Belarusian State University of Informatics and Radioelectronics, Republic of Belarus

Received April 17, 2024

Abstract. This study presents a comprehensive analysis of human gait balance using plantar pressure sensors. The research aimed to enhance the understanding of gait mechanics through detailed pressure data obtained from various activities performed by healthy male subjects. Using plantar pressure sensors and *IMU* sensors, the study captured pressure distribution across multiple foot regions during a variety of controlled indoor activities. Advanced data analysis techniques, such as recurrence plots and similarity scoring between sensor positions, were employed to assess the stability and symmetry of gait patterns. The findings highlight the potential of plantar pressure sensors in identifying gait imbalances and contributing to personalized medical interventions.

Keywords: gait parameter, plantar pressure sensor, gait balance, recurrence plot.

Introduction

As society faces the challenges of an aging population and increasing sports related injuries, the study of human gait has received widespread attention. Gait balance is a key factor in assessing and maintaining an individual's ability to walk and is essential for preventing falls and related injuries. Plantar pressure sensors, as an effective technical tool, can provide a detailed understanding of pressure distribution throughout the gait cycle, helping researchers and medical professionals understand the mechanisms of gait stability and human movement.

Currently, many researchers have made progress in studying human balance using a variety of wearable sensors, such as algorithms based on computer vision [1] and algorithms based on acceleration sensors [2]. However, these algorithms primarily perform posture estimation and do not intuitively reflect gait parameters. Therefore, we systematically analyze and evaluate human gait balance using plantar pressure sensors, paying particular attention to the pattern of pressure changes throughout the gait cycle. This study will collect plantar pressure data from various subjects to analyze its correlation with gait stability.

In summary, this study aims to provide data analysis for the assessment and intervention of gait balance using plantar pressure sensor data. By delving into the potential of plantar pressure sensor technology, we expect to open up new research directions and application prospects.

Dataset analysis

The pressure sensor data in this paper are obtained from dataset [3]. These plantar pressure sensors are positioned at eight common pressure points across the plantar foot, including the heel, arch, metatarsal, and under the big toe, providing comprehensive coverage of locations where plantar pressure changes most dramatically during movement, as illustrated in the following Figure 1. In the dataset were collected from 30 healthy male subjects aged from 20 to 25 years, with no history of limb injury. Each subject wore shoes equipped with plantar pressure sensors, and *IMU* sensors were attached to various body parts including the head, arms, wrists, chest, right side pocket of pants, and upper shin side. Participants were then instructed to engage in 21 different indoor activities within a home environment. Researchers encouraged them to perform these activities as naturally as possible, mimicking their daily routines. The activities included falling, brushing teeth, washing face, slicing, eating, washing dishes, folding clothes, sweeping, mopping, toileting, window cleaning, drinking water, hanging out clothes, ironing, using the computer, watching *TV*, jogging, walking, cycling, writing, and playing with a phone. As outlined in Table 1 below, the table enumerates the number and percentage of well segmented activity samples captured by the plantar pressure system in the dataset. Following the removal of noisy data, including transitional activities between different tasks.

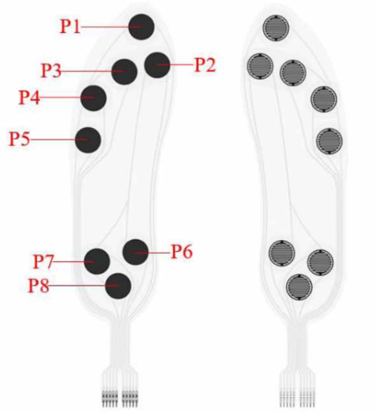

Figure 1. The planter pressure sensor

Table 1. **Activity segmentation and distribution**

Activity Categories	Number of Samples	Distribution	Activity Categories	Number of Samples	Distribution
Falling	1664	0,042	Toileting	1910	0,048
Brushing teeth	1934	0,049	Window cleaning	1897	0,048
Washing face	1917	0,048	Drinking water	1901	0,048
Slicing	1895	0,048	Hanging out clothes	1760	0,044
Eating	1899	0,048	Ironing	1794	0,045
Washing dishes	1919	0,048	Using the computer	2025	0,051
Folding clothes	2066	0,052	Watching *TV*	1945	0,049
Sweeping	1867	0,047	Jogging	1873	0,042
Mopping	1876	0,047	Walking	1906	0,042
Toileting	1910	0,048	Window cleaning	1897	0,048

Through data analysis, we display boxplots for all actions, as shown in the Figure 2. The figure presents boxplots for different activities, each measured by eight pressure sensors. The horizontal axis indicates the numeric values, representing the pressure data by the sensors, while the vertical axis labels the sensors numbered 1 to 8. For activities like using computer and watch *TV*, the sensor readings show a wide range of values, with some outliers indicating instances of high pressure. In contrast, activities like run and drink display a narrower spread and lower median values, suggesting less variation in sensor readings. The presence of outliers in activities such as wash face and play phone suggests that there were occasional high values during these activities.

We also have generated heatmaps of the sensors' placements for walking, running, falling, and cycling, as depicted in Figure 3.

These heat maps depict the average pressure distribution of smart insoles during various activities. Smart insoles typically incorporate multiple pressure sensors across different areas to monitor and record the pressure variations in the foot during various movements.

Starting with the top left heat map, during running, the sensor positions $P3$ and $P4$ show the highest average pressure values, at 792 and 612 respectively, indicating that these areas of the foot endure the most pressure while running. This may suggest that the middle part of the foot is the primary pressure point during this activity.

The bottom left heat map displays the pressure distribution while cycling. The distribution is relatively even, but the pressure peaks at sensor position $P8$ with a value of 560, possibly indicating that the force on the pedal is concentrated on the lateral side of the insole.

The top right heat map represents the pressure distribution during a fall, with $P3$ and $P5$ showing higher pressure readings of 354 and 365, respectively. This indicates that these areas receive a significant impact during a fall.

Lastly, the bottom right heat map corresponds to walking, where $P4$ and $P8$ positions register the highest pressures at 505 and 441, respectively. This could mean that the middle and the outer side of the foot are the first to make contact with the ground during walking.

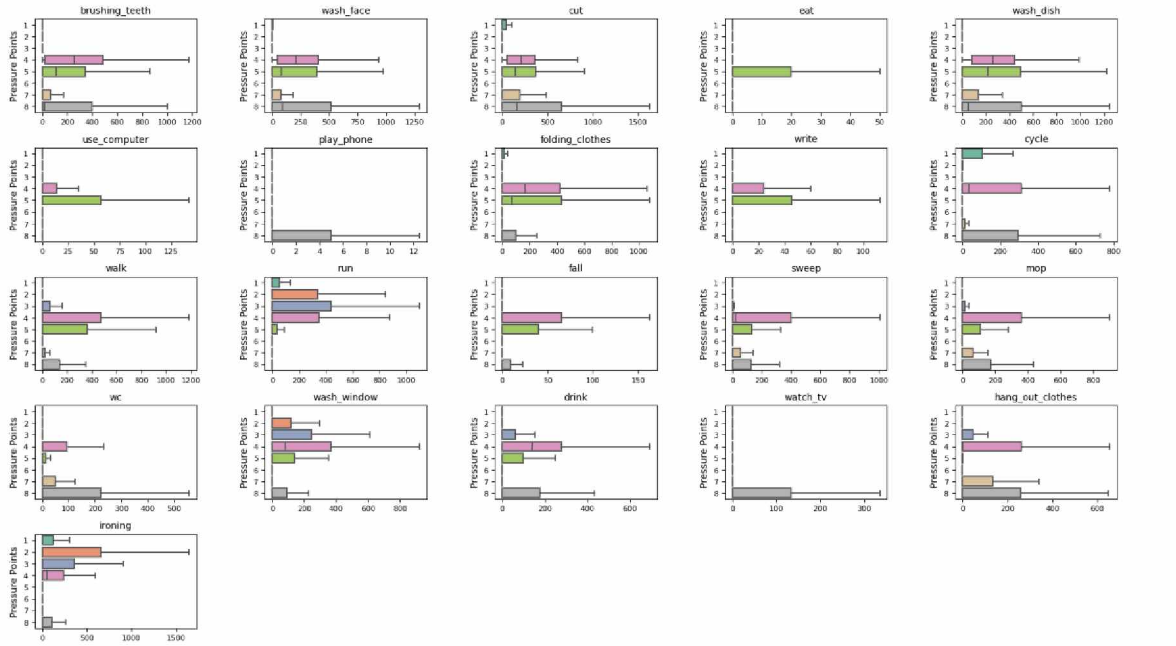

Figure 2. The boxplot of all activities for all plantar pressure sensors

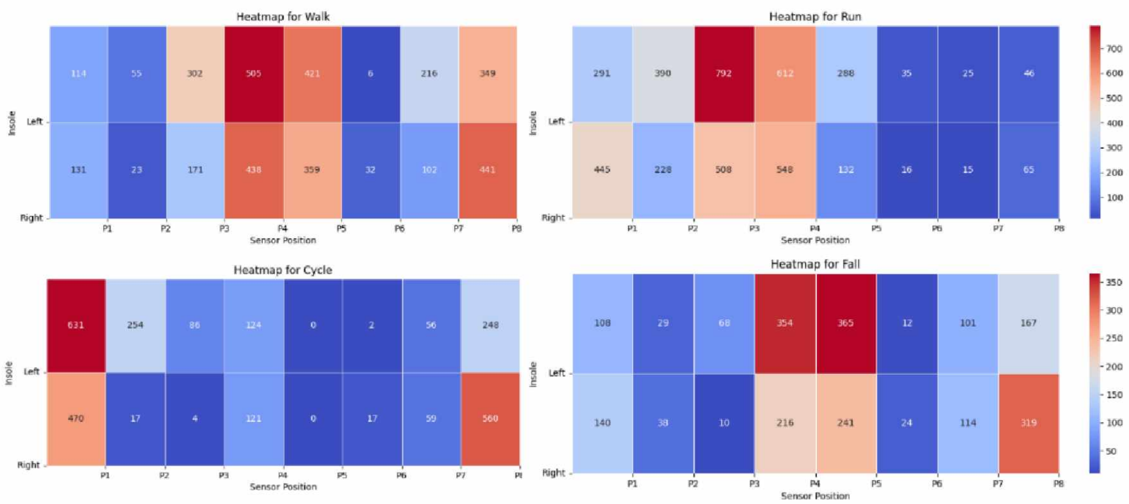

Figure 3. Heat map of average pressure for different movements of smart insoles

Gait balance analysis based on plantar pressure sensors

Gait balance analysis utilizing plantar pressure sensors offers a quantitative method to assess the stability and symmetry of walking patterns. By mapping the distribution of force across the foot during motion, these sensors provide detailed data on the biomechanics of gait.

1. Gait balance based on Recurrence plot (*RP*).

The Recurrence Plot (*RP*), developed by Eckmann [4], is one of the image encoding techniques for time series data. This visualization method illustrates the recurrence behavior between time points, highlighting patterns such as periodicity or irregular cyclicity, which are typical in nonlinear dynamical systems. Recently, *RP* has found widespread application in deep learning to convert univariate time series data into images. The *PR* formula is shown as

$$PR_L(i,j)=\begin{cases}1 \text{ if } \|p_{Li}-p_{Lj}\|\le T \\ 1 \text{ else}\end{cases}, \tag{1}$$

$$PR_R(i,j)=\begin{cases}1 \text{ if } \|p_{Ri}-p_{Rj}\|\le T \\ 1 \text{ else}\end{cases}, \tag{2}$$

$$P_L=\{p_{L1},p_{L2}\cdots p_{LN}\}, \tag{3}$$

$$P_R=\{p_{R1},p_{R2}\cdots p_{RN}\}, \tag{4}$$

where p_L and p_R are the time series pressure data of the left and right insoles. $k=0,1,2...255$, N is the number of time samples of the insole signal. T is threshold, $\|\bullet\|$ is norm function. Here, we show the *RP* transformed image using the *P*4 sensor data from walking as an example, as illustrated in Figure 4.

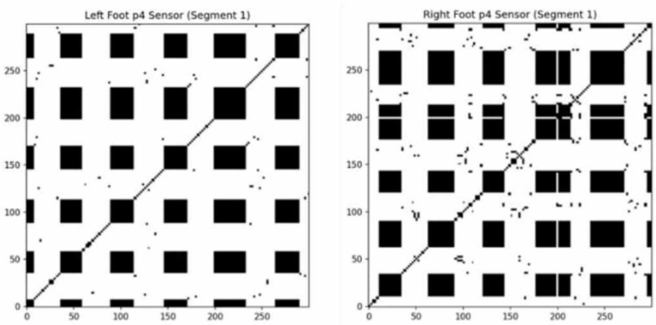

Figure 4. The *PR* transformed image based on pressure sensor during walking

When we get the recurrence plot, we use histogram calculation to calculate the similarity of the pictures of the left and right feet. The formula is as follows

$$Similarity_{L.R}=\sum_{k=0}^{255}\min(H_{normL}(k),H_{normR}(k)), \tag{5}$$

$$H_{norm}(k)=\frac{H(k)}{N_{total}}, \tag{6}$$

$$H_{total}=N\times N, \tag{7}$$

$$H(k)=\sum_{i=1}^{N}\sum_{j=1}^{N}1_{\{IRP(i,j)=k\}}, \tag{8}$$

where $k=0,1,2...255$, $IRP(i,j)$ is the intensity of the pixel at the position (i,j) in the image. $N\times N$ is the size of the image, and 1 is the indicator function, which is 1 if $IRP(i,j)=k$ and 0 otherwise. The similarity of different actions across various sensors is presented in Table 2.

Table 2. **The similarity of different activities across various sensors**

Sensors and activity	Similarity
Left walk *p*4 and right *p*4 walk	0,97
Left walk *p*4 and right *p*2 walk	0,39
Left walk *p*4 and right *p*6 walk	0,65
Left walk *p*5 and right *p*4 run	0,68
Left run *p*3 and right *p*3 run	0,94
Left walk *p*3 and right *p*4 run	0,82

The Table 2 presents a comparison of similarity scores between different activities and sensor positions for left and right sides, presumably in a smart insole context. A similarity score close to 1 indicates a high degree of resemblance in pressure patterns between the two compared activities or sensor positions.The highest similarity score is between the left and right $p4$ sensors during walking (0,97), which suggests that the pressure distribution pattern is almost identical on both the left and right sides of the body when the foot contacts the ground at position $p4$. In contrast, the left walk $p4$ and right $p2$ walk have a similarity score of 0,39, indicating a low resemblance, which could be due to different parts of the foot being used or a natural asymmetry in gait. A moderate similarity is observed between the left walk $p4$ and right $p6$ walk (0,65), which could indicate that these sensor positions, while not identical, still share some common pressure characteristics during walking. Cross activity comparisons, like left walk $p5$ and right $p4$ during running, show a similarity of 0,68, suggesting a moderate correlation, possibly because similar forces are applied to these positions across walking and running. High similarity is found between the same sensor position during the same activity on opposite sides, such as left run $p3$ and right $p3$ run (0,94), implying consistent pressure patterns during running, which is expected in a well balanced gait. Lastly, left walk $p3$ and right $p4$ run have a similarity of 0,82, which is quite high considering they are different activities. This could indicate that certain aspects of the gait, like the transfer of weight or foot roll, are maintained across walking and running.

2. Gait balance based on gait parameters.

2.1. Average contact time (*ACT*) is a crucial metric in gait analysis, reflecting the duration for which the foot remains in contact with the ground during a step. It is an indicator of gait stability and efficiency, where longer contact times may suggest a more deliberate gait, while shorter times may indicate a brisk, possibly less stable gait. The calculation of *ACT* involves recording the start and end times of contact for each step during a walk and averaging these across the number of steps taken (*NS*). The formula for *ACT* is

$$ACT = \frac{\sum_{j=1}^{NS} (T_{end,j} - T_{start,j})}{NS}, \tag{9}$$

where NS is the number of steps, $T_{end} = time(p_i = 0, p_{i-1} > 0)$.

2.2. Step frequency (*SF*) is a measure of how many steps a person takes per minute and is an important parameter in assessing walking and running patterns. It is determined by dividing the total number of steps taken by the total time of the walking or running session, which provides insight into the cadence of a person's gait. A higher step frequency can indicate a quicker, more agile gait, while a lower frequency may reflect a slower, more measured pace. The formula for *SF* is

$$SF = \frac{NS}{T_{total}} \times 60, \tag{10}$$

where NS is the number of steps, T_{total} is the total time (minutes).

2.3. Gait cycle duration (*GCD*), also known as the complete cycle duration, represents the full cycle of a gait from the initial contact of one foot to the next contact of the same foot. This duration encompasses both the stance phase, where the foot is in contact with the ground, and the swing phase, when the foot is in motion. The *GCD* is pivotal for analyzing the overall rhythm and timing of a person's walk, with implications for identifying gait abnormalities or the effects of rehabilitation. The formula for *GCD* is

$$GCD = ACT \times 2, \tag{11}$$

where ACT is the average contact time, which is the time one foot is in contact with the ground during a single step.

2.4. The average single support phase duration (*ASPD*) is an important gait parameter that represents the average time period within a gait cycle where only one foot is in contact with the ground. This phase is crucial for understanding balance and weight transfer during walking or running. The *ASPD* is calculated by summing the durations of the single leg support phases for each step and then dividing by the total number of steps, providing a mean value that reflects the stability and efficiency of a person's gait. The formula for *ASPD* is

$$ASPD = \frac{\sum_{j=1}^{NS}(T_{sg}(j))}{NS}, \tag{12}$$

where T_{sg} is the duration of the single leg support phase for step j.

In the Table 3 lists the gait parameters for both left and right feet of different users. Various gait parameters are enumerated in the table, primarily aiming to detect the balance of users' gait by observing whether the parameters of the left and right feet are balanced.

Table 3. **Comprehensive gait analysis metrics for left and right foot dynamics**

Subjects	Gait parameters									
	ACT		*SF*		*GCD*		Average peak		*ASPD*	
	Left	Right	Left	Right	Left	Right	Left	Right	Left	Right
01	1060	1139	56	52	2120	2279	1227	1164	462	540
02	1114	1126	53	53	2228	2252	1027	1193	470	461
03	1145	989	52	60	2290	1978	1804	1483	422	290
04	1361	1258	44	47	2722	2517	1491	1719	624	420
05	1069	2021	56	58	2139	2042	1429	1516	414	291
06	1045	1087	57	55	2090	2175	1127	986	354	295
07	1085	1350	55	44	2170	2701	894	565	494	882
08	994	1094	63	55	1889	2189	1411	1282	183	378
29	1027	2063	58	29	2054	4126	575	192	478	1837
30	1129	1097	53	54	2258	2194	733	603	432	572

Table 3 provides a comparative analysis of key gait parameters for both the left and right feet across different subjects, aiming to identify gait imbalances. It includes metrics such as *ACT*, *SF*, *GCD*, average peak pressure, and *ASPD*. Substantial differences between the left and right foot parameters, such as the *ACT* in Subject 05 (1069 left and 2021 right), clearly indicate an imbalance in gait symmetry. Such disparities are critical for diagnosing biomechanical abnormalities and can guide interventions for improving gait stability and efficiency.

Conclusion

The research detailed in this paper significantly advances the understanding of human gait dynamics through the application of plantar pressure sensors. Our analysis successfully demonstrated the ability of these sensors to map the force distribution across the foot during various activities, providing invaluable insights into the biomechanics of human movement. The use of recurrence plots allowed for a nuanced representation of temporal patterns, offering a new perspective on the consistency and variability of gait cycles among different individuals. Importantly, the similarity assessments across various activities and sensor positions revealed critical insights into the symmetrical and asymmetrical aspects of gait, which are vital for diagnosing and treating gait related disorders.

References

1. Jiang P., Ergu D., Liu F., et al. // Procedia Computer Science. 2022. Vol. 199. P. 1066–1073.
2. Li H., Ma J., Ren X., et al. // Pattern Recognition and Information Processing. 2023. P. 169–175.
3. Luo B., Qiu Q., Zhu T., et al. // International Conference on Intelligent Information Processing. Cham: Springer Nature Switzerland. 2024. P. 87–100.
4. Casdagli M. C. // Physica D: Nonlinear Phenomena. 1997. Vol. 108(1–2). P. 12–44.